



## Fabrication of Nanomaterials on Porous Anodic Alumina Template Using Various Techniques

Naveen Verma\*, Krishan Chander Singh, Jitender Jindal

Department of Chemistry, Maharshi Dayanand University Rohtak, Rohtak - 124 001, Haryana, India.

Received: 31<sup>st</sup> March 2015; Revised: 2<sup>nd</sup> April 2015; Accepted: 11<sup>th</sup> April 2015

### ABSTRACT

Porous anodic aluminum oxide film is a versatile template for the fabrication of nanomaterials. Porous alumina can be fabricated electrochemically through anodic oxidation of aluminum by self-organization method yielding highly ordered arrays of nanoholes. Various techniques such as chemical vapor deposition, electrodeposition, spin coating, dip coating, physical vapor deposition are elaborated for the fabrication of nanomaterials using porous anodic alumina as template.

**Key words:** Porous anodic alumina, Chemical vapor deposition, Physical vapor deposition, Spin Coating, Dip coating, Electrodeposition.

### 1. INTRODUCTION

In today's world, in the vast and rapidly growing nanotechnology fields, a bottom-up manufacturing using template materials becomes increasingly important [1]. One of the best and most widely used methods to ensure high repeatability and high quality of produced nanostructures is applications of porous anodic aluminum oxide as a template. Since Masuda and Fukuda [2] have invented the two steps method for the production of well-ordered anodic aluminum oxide (AAO) in 1995. Scientists are working on improving its manufacturing process. Usually, the highly ordered porous anodic alumina is obtained as a result of self-organized two-step anodization of pure aluminum pieces in various acidic solutions or in some other electrolyte. The most commonly and widely used electrolytes, to produce nanosized pores in the range of 10-240 nm, are the acidic electrolytes like oxalic acid, sulfuric acid, phosphoric acid or their combinations. It has been found that the best honeycomb-like structure of anodic alumina layers in which uniform pore arrangement and uniform size distribution obtained is produced in sulfuric acid electrolyte [3]. However, based on the calculations of regulatory ratio, the best honeycomb-like structure of nanopores is obtained in the oxalic acid solutions [4]. There are various anodizing parameters such as applied voltage, solution temperature, electrolyte concentration affect the control of pore diameter of AAO [5-7]. The AAO is used as template for the growth of self-organized, highly ordered nanodots,

nanorods, nanotubes, and various other nanomaterials which are useful. Various techniques are used for the production of nanomaterials.

### 2. CHEMICAL VAPOR DEPOSITION (CVD)

CVD is a chemical process used to produce high-purity, high-performance solid materials. The process is generally used in the semiconductor industry to produce thin films. In this technique, the substrate is exposed to one or more volatile precursors which react or decompose on the substrate surface to produce the desired deposit. CVD is widely used in the microfabrication processes to deposit materials in different forms including mono crystalline, polycrystalline and amorphous. CVD of materials in nanoporous holes of alumina is a very important and challenging topic for researchers. Since it is interesting to investigate the filling of high aspect ratio of holes which are contained by porous alumina film. When a thin porous alumina film is uniformly coated with carbon, the carbon coated film exhibits a bright, and tunable interference color with much higher saturation than the primary alumina membrane. Chemical vapor synthesis (CVS) is a modified CVD method where the process parameters are adjusted to form nanoparticles instead of the film. Both in CVD and CVS, precursors are metal organics, carbonyls, hydrides, chlorides, and other volatile compounds in gaseous, liquid or solid state. The major limitation of the CVS process is the availability of appropriate precursor materials.

\*Corresponding Author:

E-mail: vermanaveen17@gmail.com

The energy for the conversion of the reactants into nanoparticles is supplied in hot wall (external furnace), flame (reaction enthalpy), plasma (microwave or radio frequency), and laser (photolysis or pyrolysis) reactors. The most important process parameters determining the quality and usability of the nanopowders are the total pressure (typical range from 100 to 100000 Pa), the precursor material (decomposition kinetics and ligands determining the impurity level), the partial pressure of the precursor (determining the production rate and particle size), the temperature or power of the energy source, the carrier gas (mass flow determining the residence time), and the reactor geometry. The nanoparticles are extracted from the aerosol by means of filters, thermophoretic collectors, and electrostatic precipitators or scrubbing in a liquid [8,9]. A more developed CVD technique called as plasma enhanced CVD is one of the bright methods for the growth of carbon nanotubes using porous AAO as template. A controllable method for carbon nanotubes production is plasma enhanced-CVD. The processes involve the growth at low temperature and provide easy vertical alignment to the nanomaterials. Plasma is a partially ionized gas consisting of electrons and ions. Typical ionization fractions of  $10^{-5}$  to  $10^{-1}$  are encountered in process reactors. Plasmas are electrically conductive with the primary charge carriers being the electrons. The light mass of the electron allows it to respond much more quickly to changes in the field than the heavier ions. For example, the thermal CVD of silicon nitride occurs between 700°C and 900°C, the equivalent PECVD process is accomplished between 250°C and 350°C. The carbon nanotubes were grown by PECVD on the AAO template at 550°C temperature. The ethylene ( $C_2H_2$ ) is used as a carbon source and the ammonia ( $NH_3$ ) gas used for dilution purpose and as a catalytic gas. For the growth of CNTs, the thorough hollow porous membrane was prepared by removing its barrier layer. Plasma CVD has numerous advantages over thermal CVD. Obviously the reduced deposition temperature is a bonus for the semiconductor industry which must worry about dopant diffusion and metal interconnects melting at the temperatures required for thermal CVD. Furthermore, the low pressures (between 0.1 and 10 Torr) required for sustaining a plasma result in surface kinetics controlling the reaction and therefore greater film uniformity. A disadvantage of plasma CVD is that it is often difficult to control stoichiometry due to variations in bond strengths of various precursors. For example, PECVD films of silicon nitride tend to be silicon rich because of the relative bond strength of  $N_2$  relative to the Si-H bond. In addition, some films may be easily damaged by ion bombardment from the plasma. Tungsten oxide was deposited on the PAA template and macroporous silicon substrates via aerosol assisted CVD from the precursor tungsten hexaphenoxide [10]. The results show that the thin porous anodic alumina substrates have potential

as templates for growing microstructured tungsten oxide films and macroporous silicon substrates cause the growth of “grids” of polycrystalline tungsten oxide. The effect of interstitial lattice mismatch upon  $Hg_{1-x}Cd_xTe$  epitaxial layers grown by metal organic CVD (MOCVD) were investigated [11].  $HgCdTe$  was found to be easily affected by lattice mismatch of less than  $\pm 0.1\%$  [12].  $\alpha-Fe_2O_3$  thin film were fabricated by aerosol assisted CVD using a hexanuclear iron precursor ( $Fe_6 [PhCOO]_{10} [acac]_2 [O]_2 [OH]_2$ ).  $3C_7H_8$  [13] where PhCOO-benzoate and acac- 2, 4-pentanedionate). The Si-doped  $\alpha-Fe_2O_3$  was prepared by atmospheric pressure CVD (APCVD) with iron pentacarbonyl ( $Fe [CO]_5$ ) as iron precursor and tetraethoxysilane as the Si precursor at 450°C. A requirement of APCVD process is that the precursor material must have high enough vapor pressure [14].

Silver nanowires were fabricated by deposition in the porous anodic alumina nanochannels with almost 100% efficiency only with small fluctuations in the growth rate. The monocrystalline silver nanowires growth direction is perpendicular to  $\langle 110 \rangle$  direction and the diameter is varied from 30 nm to 70 nm depends on how the alumina template is prepared. For the fabrication of uniform porous alumina layer pulsed electrodeposition and a highly conductive electrolyte are prerequisite conditions [15]. Electrodeposition of ZnO on the porous anodic alumina membrane (PAAM) with a sputtered Au electrode yields polycrystalline ZnO nanotubes. The deposition of particles starts at the Au cathode on the bottom of nanopores and the deposition time control the length of ZnO nanotubes. These technologies provide a new way to fabricate metal oxide nanotube array and have applications in optoelectronics and sensing devices [16].

Few transition metal complexes like iridium (Ir), Platinum (Pt), Rhodium (Rh), or Palladium (Pd) have a favorable combination of stability, volatility, and clean decomposition. For this group of metals, the rates of deposition are low. So the use of auxiliary energy sources such as plasma or laser to assist CVD is a viable route to increase deposition rates [17].

Catalysis is the main part of CVD-CNT technique. With the use of a suitable catalyst; the CVD temperature can be brought down to room temperature and also possible to control the diameter and chirality of the resulting CNTs [18].

Fabrication of  $CeO_2$ -doped  $Y_2O_3$ -stabilized  $ZrO_2$  films on dense silicon and porous alumina substrates were produced via atmospheric pressure metal organic CVD. A toluene solution of the precursors Zr ( $tfac$ )<sub>4</sub>, Y ( $hfac$ )<sub>3</sub>, and Ce ( $tmhd$ )<sub>4</sub> was used to deposit films with thickness around 1  $\mu m$ . The results show that crystalline multicomponent films can be obtained and that solution composition can be manipulated to

change film composition. Deposition temperature and precursor concentration have important effects on the film morphology and deposition rate [19].

An alternative method for the common use of oxalic acid, acetylene pyrolysis in porous alumina template obtained by anodic oxidation in sulfuric acid solution can produce carbon nanotubes with a higher density ( $\sim 56 \times 10^9 \text{ cm}^{-2}$ ) at 650°C and 550°C. After boiling in water, carbon nanofibers can be obtained in the templates anodized in oxalic acid solution by growing at 650°C through the CVD method which shows the catalytic activity for anodic alumina. No carbon tubes or carbon nanofibers can be formed if the CVD temperature decreases to 500° [20].

Catalytic CVD-either thermal [21] or plasma enhanced is the standard method for the CNTs production. CCVD is an economically executable process on the large scale for the production of pure CNTs. The function of the catalyst in the CVD process is the decomposition of carbon source via either plasma irradiation (plasma enhanced CVD) or heat (thermal CVD) and its new nucleation to form CNTs. The most frequently used catalysts are transition metals Fe, Co, Ni, and Au [22,23] and mostly some hydrocarbons like methane, ethane, ethylene, xylene or ethanol are used as a carbon source in CVD. CNTs growth efficiency depends upon reactivity and concentration of gas-phase intermediates when gaseous carbon source used for the growth of CNTs. The choice of catalyst is one of the most important parameter affecting the CNTs growth.

Flahaut et al. [24] reported that the catalyst was prepared by the combustion route using either urea or citric acid for the synthesis of CNTs by CCVD. Xiang et al. prepared CNTs via CCVD of acetylene on a series of catalysts derived from Co/Fe/Al layered double hydroxides. Lyu et al. [25] produced high quality and high purity DWNTs by catalytic decomposition of benzene as an ideal carbon source and Fe-Mo/Al<sub>2</sub>O<sub>3</sub> as a catalyst at 900°C. Jiang et al. [26] studied the growth of CNTs in situ on the pre-treated graphite electrode via CCVD using Ni(NO<sub>3</sub>)<sub>2</sub> as the catalyst [27]. The prepared CNTs had 80 nm and 20 nm in outer and inner diameter, respectively. Feng et al. used acetone as a carbon source, ferrocene as a source of Fe catalyst and thiophene as a promoter to synthesize high-quality DWNTs thin films through CCVD [27]. Kim et al. [28] gives a royal method for the growth of CNTs that uses three different iron-containing proteins; hemoglobin, myoglobin, and cytochrome C in order to control precisely the size and structure of CNTs. These iron-containing protein source were adsorbed on the amine-terminated self-assembled monolayer (SAM) surfaces by peptide bonds between the carboxyl groups of the proteins and the amine groups of the SAMs and used

directly as catalysts in the synthesis of CNTs. Plasma enhanced CVD is a suitable method for the synthesis of CNTs and modification of their surface properties. Lim et al. [29] gives the application of PECVD in the production and modification of CNTs. PECVD used in several different modes; radiofrequency (RF-PECVD), direct current (DC-PECVD), diffusion (D-PECVD), and microwave (MW-PECVD). Kim and Gangloff demonstrated the low temperature (480°C-612°C) synthesis of CNTs on different metallic under layers (i.e., Ir, Ag, Pt, W, and Ta) using diffusion PECVD [30].

### 3. ELECTRODEPOSITION TECHNIQUE

Electrodeposition is a very versatile tool to fabricate multi-component metal oxide nanotube array composites. Mainly electrodeposition technique refers in three processes. Electroplating, a process that uses electrical current to reduce dissolved metal cations, so that they form a coherent metal coating on an electrode. Electroplating uses an electrical current to finish a contact or component with a thin layer of metal. The applications of electroplating deposits have a desired property like abrasion, wear resistance, corrosion protection, lubricity or esthetics onto a substrate lacking the desired property. The electroplating process is also known as electrodeposition. It is a galvanic or electrochemical cell acting in reverse. The part being plated becomes the cathode of the circuit. With a soluble anode, the anode is made of the metal to be placed on the part which dissolves in a chemical solution, like gold or palladium. In a soluble anode, the metal is actually contained in the solution. Both the anode and the part or cathode is submerged in a solution containing one or more metal salts in addition to other ions that enable the flow of electricity throughout the solution. A rectifier supplies direct current to the cathode causing the metal ions in solution to lose their charge and plate onto the part or cathode within the solution. As the electrical current flows through the solution, the anode dissolves in a controlled manner and replenishes the ions in the bath. Electrophoretic deposition, a term for a broad range of industrial processes which includes electrocoating, e-coating, cathodic electrodeposition, anodic electrodeposition, and electrophoretic coating, or electrophoretic painting. Under potential deposition, a phenomenon of electrodeposition of a species (typically reduction of a metal cation to a solid metal) at a potential less negative than the equilibrium (Nernst) potential for the reduction of this metal.

Embedded thin layer of titanium between the porous anodic alumina template which is supported on a Si substrate, is used for the fabrication of vertical arrays of high aspect ratio (>100) InSb nanowires with diameters of ~20 nm. SEM results show that the InSb nanowires completely fills the channels of the porous anodic alumina thereby acquiring a wire diameter of about 20 nm. Raman spectrum of the InSb nanowires indicates high crystal quality [31].

Highly ordered ZnO nanowires array were fabricated by the oxidation of metal Zn that was electrodeposited in the pores of anodic alumina membrane [32]. The ZnO nanowires diameter is in the range from 15 nm to 90 nm. Atomic force microscopy, X-ray diffraction (XRD), and transmission electron microscopy (TEM) characterization shows that the polycrystalline ZnO nanowires array were uniformly assembled into the hexagonally arranged nanochannels of the anodic alumina membrane. In this work, the arrays of semiconductor ZnO nanowire were synthesized by oxidizing Zn that was electrodeposited in the pores of AAMs. As a wide band gap semiconductor, ZnO is of interest for low voltage and short wavelength electro-optical devices such as light emitting diodes (LED) and diode lasers. ZnO nanoparticles offer considerable potential as starting material for other applications such as transparent ultraviolet protection films and chemical sensors. The uniform orders of ZnO nanowire arrays make it more practical to apply ZnO in electron devices and chemical sensors.

Zinc telluride is an important semiconductor material with a direct optical band gap of 2.2-2.3 eV at room temperature, which has potential applications in optoelectronics and thermoelectric devices [33]. A plating solution containing cadmium sulfate, tellurium dioxide, and citric acid was used to obtain thin films of zinc telluride by electrodeposition into AAM pores. From this study, it was possible to establish the optimal experimental conditions for the preparation of zinc telluride films with an almost stoichiometric atomic composition (50.40% Zn, 49.60% Te). The ZnTe nanowires on the AAM membranes with 50 nm of pore diameter were also fabricated through potentiostatic electrodeposition under similar conditions.

Synthesis of silver telluride nanowire arrays were carried out by cathodic electrolysis on the porous anodic alumina template from dimethyl sulfoxide (DMSO) solutions which contain 0.1 M  $\text{NaNO}_3$ , 5.0 mM  $\text{AgNO}_3$  and 6.0 mM  $\text{TeCl}_4$  [34]. Synthesized  $\text{Ag}_2\text{Te}$  nanowires are well crystallized monoclinic that obtained at potentials between -0.55 to -0.65V. By the adjustment of the concentration of  $\text{TeCl}_4$  in the solution, the chemical composition of the silver telluride nanowires can be controlled. The method of using DMSO as a solvent and  $\text{TeCl}_4$  as a Te source could be extended to the synthesis of other metal telluride by electrodeposition.

Fabrication of copper nanowires [35] with diameter 100 nm and 200 nm in an electrochemical cell takes place through electrodeposition technique based on the principle of electroplating using anodic alumina and polycarbonate templates. Electrochemical deposition route is easy, low cost as well as cumbersome

compared to other fabrication techniques, namely pulsed laser deposition, vapor liquid solid (VLS) method, and CVD [36]. Electrodeposition of copper nanowires depends on many factors, namely inter-electrode spacing, electrolyte composition and pH value, current density and time of deposition. The diameter of copper nanowires nearly matches with the pore diameter of polycarbonate template, but the wire growth is not as perfect cylinders. The aspect ratio is in the order of 300.

Electrodeposition of ZnO on the PAAM with a sputtered Au electrode yields polycrystalline ZnO nanotubes. The deposition of particles starts at the Au cathode on the bottom of nanopores and the deposition time control the length of ZnO nanotubes. This technology provides a new way to fabricate metal oxide nanotube array and have application in optoelectronics and sensing devices [16]. Different nanostructures of metal and alloys can be fabricated by electrodeposition technique using anodic alumina membrane as template. Nickel and copper oxide electrodeposition resulted in the formation of short metal nanotubes of nickel about 5  $\mu\text{m}$  long and large array of aligned copper (I) oxide nanowires, respectively. Potential perturbation and bath composition influence the composition and crystallographic nature of  $\text{Cu}_2\text{O}$  nanowires.  $\text{CeO}_2$  nanotubes and  $\text{PbO}_2$  nanowires also fabricated by electrodeposition techniques, former from non-aqueous electrolyte and later by potentiostatic electrodeposition under anodic polarization [37]. For the fabrication of Ni nanotubes, nickel electroless deposition was carried out in a bath containing Ni sulfate. Under a square potential waveform, Ni NTs were fabricated inside the channels of anodic alumina membranes and in the trapezoidal wave; length of nickel nanowires increased with deposition time [38]. Sn-Co nanowires also obtained by electrochemical deposition which is carried out at -1.0 V (SCE) and 60°C in a solution of 0.005 M  $\text{CoSO}_4$  and 0.01 M  $\text{SnSO}_4$  in the presence of 0.2 M  $\text{Na}_2\text{SO}_4$  as supporting electrolyte and 0.2 M sodium gluconate as chelating agent [38]. By adjusting the deposition time, nanowires of different composition and length were formed. Metal oxide nanostructures like  $\text{Cu}_2\text{O}$ ,  $\text{CeO}_2$  and  $\text{PbO}_2$  are obtained by template electrodeposition. For the fabrication of  $\text{Cu}_2\text{O}$  nanostructures, the electrodeposition was carried out at 55°C and electrode potential of -0.2 V (SCE). Two different electrolyte solutions were used: The first was a 0.01 M cupric acetate/0.1 M sodium acetate bath at pH=6.5 and the 2<sup>nd</sup> plating bath was prepared by dissolving 0.4 M  $\text{CuSO}_4$  in a 3 M lactic acid solution with pH=10 [36].

Fabrication of uniform and regular arrays of Cu and Pd nanowires by displacement deposition at room temperature. For the preparation of Cu nanowires, 0.2 M copper sulfate solution was used while a

solution containing  $\text{Pd}(\text{NH}_3)_4(\text{NO}_3)_2$  was used for the fabrication of Pd nanowires are straight, dense, and continuous with a uniform diameter through the entire length [36,39-41].

#### 4. DIP COATING

In dip coating techniques, the porous template is immersed in a colloidal dispersion of particles which wets the pores; upon withdrawal from solution and drying, some particles remain within the template [42]. Assisted dip coating methods have also been reported where a secondary force is used to aid the infiltration of particles into the template; for instance, magnetic stirring can be used to force the liquid to impinge upon the template thereby increasing the number of infiltrated particles. Dip coating methods, however, achieve at most a modest 3.5 volume percent nanoparticle filling [43] rendering them unsuitable for a complete filling of the template with building blocks and voiding any possibility of obtaining a freestanding structure upon removal of the template.

Dip Coating is a simple and low-cost method to create a thin film on a substrate. In general, it can be separated into five stages- (i) Immersion: The substrate is immersed in the solution of the coating material at a constant speed. (ii) Start-up: After the substrate has remained inside the solution for a while and we start to pull it up. (iii) Deposition: The thin film deposits itself on the substrate while it is pulled up at a constant speed. The speed determines the thickness of the coating. (iv) Drainage: Excess liquid will drain from the surface of the substrate. (v) Evaporation: The solvent evaporates from the liquid to form the thin film on the substrate.

The effect of alkali metal cations (namely lithium, sodium and potassium) on the silicate/alumina was studied in this work [44]. Porous anodic aluminum oxide were silicate treated by dipping in water based silicate solutions of different monovalent alkali metal cations ( $\text{Li}^+$ ,  $\text{Na}^+$ ,  $\text{K}^+$ ). Aqueous sodium silicate solution is widely used as cleaner and corrosion inhibitor for aluminum alloys. The alumina oxide surface modification during immersion in solution was studied as a function of the type of cation at ratio  $\text{SiO}_2/\text{M}_2\text{O}=1$  (Here  $\text{M}=\text{Li}$ ,  $\text{Na}$ ,  $\text{K}$ ) at different temperature of the silicate solutions ( $30^\circ\text{C}$  and  $70^\circ\text{C}$ ). Alkali metal cation acting as a coagulating agent between the anodized alumina surface and the silicate anions. Silicate anion coagulation would result in a homogenous adsorption of the silicate on the anodic oxide surface. Morphological differences were observed in alumina surface by changing the type of alkali metal cation after the immersion in solution. The dissolution of oxide layer was faster in potassium silicate, while the highest protection of the oxide layer was given by lithium. The three cations show different

observations due to their different size. The high degrees of hydration of lithium have faster silicate adsorption on the alumina surface than the potassium of the oxide layer from alkaline dissolution.

Maghemite ( $\gamma\text{-Fe}_2\text{O}_3$ ) with 20 nm diameter nanoparticles were filled by dip-coating process into the aluminum oxide nanotemplate pores with 100 nm diameter and their magnetic properties were studied [45]. The maghemite nanoparticles were stabilized by oleic acid. To obtain the multilayer of maghemite nanoparticles, the dip-coating procedure is repeated. The magnetic moment of AAO with particles increased in proportion of the number of layers. These results demonstrate the possibility of integrating nanoparticles into nanotemplates and controlling their properties. Ti-Al composite oxide film was obtained between  $\text{TiO}_2$  coating and Al substrate by using the sol-gel dip coating method [46]. In this process, Al specimens were covered with  $\text{TiO}_2$  film by sol-gel dip coating and then anodized in ammonium adipate solution. Characterization studies (TEM, XRD, electrochemical impedance spectroscopy) shows that dual layered anodic oxide film formed between  $\text{TiO}_2$  coating and aluminum substrate. The dual layer structure consists of  $\text{Al}_2\text{O}_3$  as an inner layer and an outer Ti-Al composite oxide layer. With the repetition of sol-gel dip coating, the thickness of inner layer reduced and outer layer increased. Pore network in  $\text{TiO}_2$  coating affect the formation and structure of Al anodic oxide film.  $\text{TiO}_2$  deposited anodic oxide film has 80% higher capacitance than that without  $\text{TiO}_2$  and the resistance decreases with the repetition of dip coating.

The inner alumina layer grew due to the inward transport of  $\text{O}^{2-}$  anions and the outer Ti-Al composite oxide layer grown due to the outward transport of  $\text{Al}^{+3}$  cations.  $\text{TiO}_2$  film caused the thickness variation of both layers by inhibiting  $\text{Al}^{+3}$  and  $\text{O}^{2-}$  ion transport during anodization.

Highly ordered  $\text{TiO}_2$  nanowires were prepared by dipping technique into a porous anodic alumina template for the application as electrolytic capacitor [47]. Homogenous infiltration of  $\text{TiO}_2$  nanowires were obtained through dipping technique even in the highly acidic solution. The electronic capacitance of the  $\text{TiO}_2$  nanowires were measured and compared with the theoretical calculations using an effective thickness, which correspond to the mean radius of nanowires.

#### 5. SPIN COATING

Spin coating is a procedure used to deposit uniform thin films to flat substrates. Usually, a small amount of coating material is applied on the center of the substrate, which is either spinning at low speed or not spinning at all. The substrate is then rotated at high speed in

order to spread the coating material by centrifugal force. Rotation is continued while the fluid spins off the edges of the substrate, until the desired thickness of the film is achieved. The applied solvent is usually volatile, and simultaneously evaporates. So, the higher the angular speed of spinning, the thinner the film. The thickness of the film also depends on the viscosity and concentration of the solution and the solvent. Spin coating is widely used in microfabrication, where it can be used to create thin films with thicknesses below 10 nm. It is used intensively in photolithography, to deposit layers of photoresist about 1  $\mu\text{m}$  thick.

Uniformly and controlled distribution of Co and Ag nanoparticles on the Si and SiO<sub>2</sub> substrate can be achieved by employing the spin coating method [48]. The particle density can be controlled by changing the molar concentration of nanoparticle colloids with the fixed rotational speed of the spin coater. Co nanoparticles were synthesized by thermal decomposition process where 4 ml of 0.5 mol (M) Co<sub>2</sub>(CO)<sub>8</sub> toluene solution was injected into hot toluene solution with 0.089 g of NaAOT (Sodium bis[2-ethylhexyl]sulfosuccinate). After refluxing for 6 h at 380 K and following centrifuge separation process, black colored Co nanoparticle were obtained in powder form. This AOT stabilized Co nanoparticle were dispersed in toluene. Ag nanoparticles were obtained by alcohol reduction of silver acetate (AgAc) in the presence of polyvinyl pyrrolidone [49].

Alumina membrane based high-quality PbO<sub>2</sub> and Pb (Zr, Ti) O<sub>3</sub> metal oxide nanowires with uniform diameter and relatively smooth surface are synthesized by combination of sol-gel processing and spin coating method [50]. The resulting fabricated PbO<sub>2</sub> nanowires have a single crystalline structure with 40 nm diameter and 10  $\mu\text{m}$  length and PZT nanowires have diameter 50 nm and length 20  $\mu\text{m}$ . Spin coating creates an outward radial flow from the center of the disk which results in the removal of the residual air inside the nanopores. The air flow can provide a suction effect for the sol to enter the nanopores, providing the coating is the versatile method that is favorable for a wide variety of sol system, regardless of the acidity of the solution [51].

A low-cost inorganic matrix contain terbium doped yttrium aluminum oxide films were synthesized by spin coating deposition grown on a silicon wafer and terbium photoluminescence was studied at annealing temperature from 400°C to 1100°C on porous anodic alumina [52]. A Tb-doped inorganic matrix on the basis of PAA as prospective for green terbium emission within the broad temperature range of applications.

For the deposition of microporous silica on anodic alumina template, a mesoporous silica layer with

2-6 nm pore size deposited on the anodized disk by dip coating. Later the mesoporous gas separation membrane layer is deposited by spin coating, obtaining a defect free mesoporous silica having high selectivity and permittivity [53]. This method can be used for the development of different type of inorganic membranes having the advantage of availability and low permittivity resistance of anodic alumina oxide template.

Synthesis of single crystalline PbO<sub>2</sub> nanowires (diameter 42 nm) carried out by a spin-coating process of putting a lead oxide sol-gel solution into a PAAM. Lead oxide has various application and most one is, use as active material of lead acid battery [54]. Other investigations show that the PbO<sub>2</sub> is a strong oxidant, like ozone, due to its high overpotential for oxygen evolution. Electron diffraction analysis and TEM results shows that the synthesized PbO<sub>2</sub> nanowires are single crystalline and orthorhombic with diameter 30 nm to 52 nm. These PbO<sub>2</sub> nanowires are very sensitive toward electron beam irradiation in the TEM microscope, resulting in the phase transformation from  $\alpha$  PbO<sub>2</sub> to  $\beta$  PbO.

## 6. PHYSICAL VAPOR DEPOSITION

PVD is the process involving vaporization of the coating material in vacuum, transportation of the vapor to the substrate and condensation of the vapor on the substrate surface. Two PVD techniques are used for depositing wear resistant alumina coatings: Sputtering is a PVD method utilizing argon ions for bombarding a cathodically connected target made of the coating material. Atoms of the target are knocked out by the high energy ions and deposit on the substrate surface. In the EB-PVD method, the target anode is bombarded in a high vacuum with an electron beam generated by a charged tungsten filament. Electron beam evaporation method is much faster than sputtering. According to the sputtering process [55] takes approximately 50 h to prepare a 0.24-0.31 mil (6-8  $\mu\text{m}$ ) thick alumina film compared to only 20 min needed for the E-beam evaporation. Typical alumina coating obtained by the Electron beam PVD methods has a columnar structure. Dense fine grain crack-free structure of PVD deposited alumina coatings does not requires post-deposition polishing and provides low wear rate. The wear characteristics of the foil air bearings are greatly improved by applying a protective sputter deposited Al<sub>2</sub>O<sub>3</sub> coating. AAO template is used for the electrodeposition of cuprous oxide (Cu<sub>2</sub>O) nanorods in alkaline (pH=12) copper sulfate electrolyte TiN coated Si wafer in room temperature [56]. In this work, electrochemical deposition method is used because length of the nanorods can be controlled by changing electrochemical factors. Cuprous oxide, a p-type semiconductor, having band gap 2.0-2.2eV has many applications in hydrogen production, superconductor, solar cell and negative electrode material [57-60].

The ordered arrays of Ni and Au nanodots with uniform diameter and density of  $1.2 \times 10^{10} \text{ cm}^{-2}$  on the anodic alumina oxide template were fabricated by a three-step method combining PVD, grazing ion milling and thermal annealing technique [61]. First, deposition of 80 nm Ni film on the AAO template, which was prepared by two-step anodization method, by ion beam sputter deposition. After that grazing ion milling used for the removal of continuous layer and lastly spherical nanodot array was formed by thermal annealing process. Above similar process is used for the deposition of Au film and resulting Au nanodot arrays are formed. The packing density of nanodots can be controlled by selecting a template with the desired pore density. Due to the high uniformity and controllability of the diameters, the nanodots are very stable for the study of their size-related properties. The diameter of the nanodots can be controlled independently of the packing density which helps for investigating the coupling between adjacent nanodots [61].

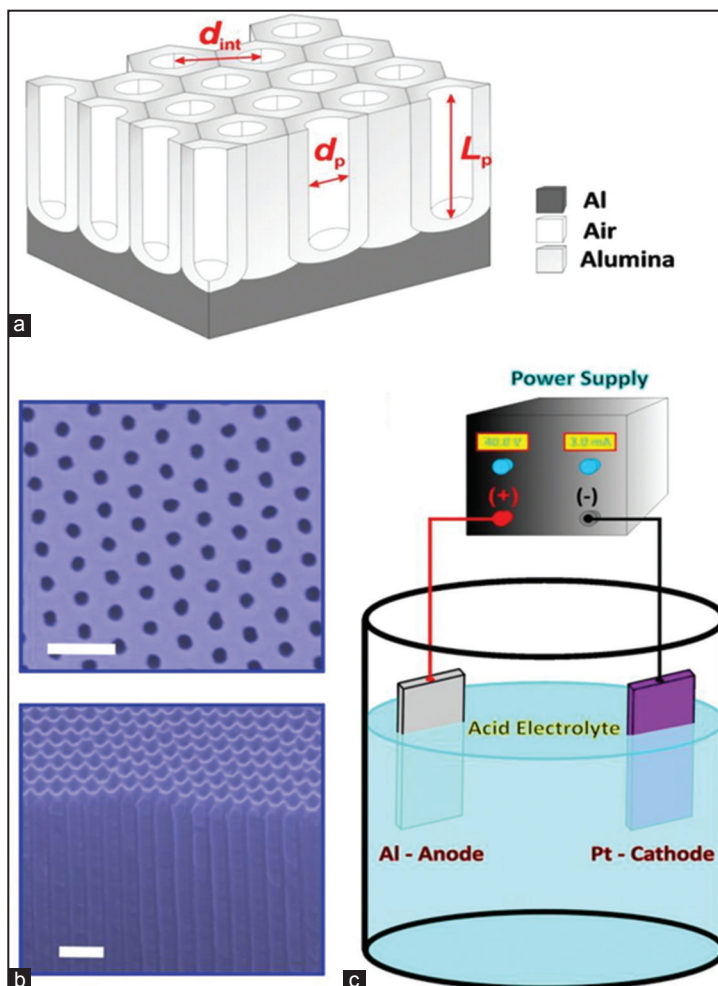
Aluminum nanotubes with pore external diameter 60 nm, inside diameter 35 nm and length 2  $\mu\text{m}$ , have

been fabricated by PVD/atmospheric pressure injection using porous anodic alumina as a template [62]. PVD is a simple and suitable method for the fabrication of special purpose of metal nanotubes and it is applicable only for those metals which are evaporated in vacuum. For fabricating metal nanotubes on AAO templates, a new method “two-step evaporating method” is developed. This method includes two evaporation steps. First step is an aluminum evaporating process for depositing Al on the surface of the porous alumina template in vacuum and the second step is a heating process of Al sample which is deposited on the surface into the pores under the atmospheric pressure.

A modern way for the fabrication of macroporous TiO<sub>2</sub> oxygen sensors as an etching mask for the production of macroporous silicon substrate is discussed by chih-cheng Lu et al. [63]. For the enhancement of sensor sensitivity and to reduce sensor dimensions, a higher specific surface area is generating with this method.

### 7. APPLICATION OF NANO MATERIALS

PAAM is used as universal nanoscale templates due to its simple preparation technique. It has been widely



Schematic diagram for the fabrication of porous anodic alumina (a) Vertical view of porous layer on anodic aluminum template, (b) Pores formed on alumina layer after anodization, (c) Experimental setup

used to fabricate nanotubes and nanowires by filling various materials into the nanopores such as metals, semiconductors, and organic matters [64-66].

A porous anodic aluminum oxide template is used for the fabrication of gold nanotube membranes (GNT). GNTs have various types of applications because the shape and structure of GNTs are closely related to their catalytic, electronic, and optical properties [67,68]. Catalytic properties of gold depend on the size of the particle and the interaction between gold and the supporting oxide [69]. Gold nanotube membranes have numerous applications including selective molecular separation, enzyme reactors, drug delivery, biosensing, and electroanalysis [70-72]. The excellent catalytic properties (catalytic rate constant  $K = 0.132 \text{ min}^{-1}$ ) of the gold nanotube membranes were demonstrated by testing catalytic conversion of 4-nitrophenol into 4-aminophenol in the presence of  $\text{NaBH}_4$  as a reductant.

Fabrication of Ni nanowires on AAO template is carried out by the combined technique of anodic anodization and direct current electrodeposition. Metal nanowires have various applications in high density recording media [73,74] and optical labels [75]. The diameter of Ni nanowires is about 30 nm which corresponds to the diameter of the pores in the alumina film. Ni nanowires exhibit a polycrystalline bamboo-like structure.

Since 19<sup>th</sup> century, carbon nanotubes are of great interest of study as the key material for nanotechnology because of their semiconducting, electron emitting, high strength and other unique properties [76,77].

Metal nanowires have various unique electrical, electronic, thermoelectrical, optical, magnetic and chemical properties. Morphology of nanowires, diameter dependant band gap and carrier density of states are the factors which influence the physical properties of MNWs. MNWs and metal nanorods have unique physical properties [36].

Semiconductor nanocrystallites [78,79] have unique electronic, optical, and catalytic properties. These are of great interest in optical and photoelectronic devices such as optical switches, lasers, and LEDs. The optical properties of nanocrystallites are very different from the bulk material. In the fabrication of semiconductor nanomaterials, the control of the size, size distribution and arrangement is of great importance in nanoelectronics, optoelectronics, and catalyst chemistry [80]. Various diameter modulated metallic nanowires (Ag, Au, Ni, and Ag-Au) were fabricated by electrodeposition in the pores of anodic alumina membrane. Nanowires made of metal; semiconductor and polymer have many novel applications ranging from chemical and biological sensors to optical, thermoelectric, and electronic

nanoscale devices [81,82]. Numerous techniques such as VLS growth, laser assisted catalytic growth, CVD, laser ablation, molecular beam epitaxy, e-beam lithography, Nanosphere lithography – assisted techniques have been used to prepare nanowires [83].

Carbon nanotubes mainly used as gas sensors due to their large surface area, high electrical conductivity, and chemical stability. Gas sensors have various novel applications [84,85]. CNT-based sensors have been used for the detection of gases such as  $\text{H}_2$ ,  $\text{O}_2$ ,  $\text{NO}_2$ ,  $\text{CO}_2$ , and  $\text{NH}_3$  [86,87] and organic compounds [88]. CVD is used in the direct synthesis of CNTs on substrate or CNT powders were posted on substrates for the fabrication of devices. The use of metallic nanostructures with high work function is beneficial for the electrical properties of the cell. The gold and silver nanodot arrays are prepared on a glass/indium tin oxide substrate using AAO lithography. This technique is very efficient for the preparation of nanostructures [2,89].

Ultra-sensitive sensing and biosensing devices using nanomaterial have great interest of study due to their unique physical and chemical properties. Self-ordering electrochemical anodization is used for the synthesis of the highly ordered vertically aligned nanoporous and nanotubular structures with well-defined and controllable geometry, which are useful for the production of such sensing and biosensing devices [90]. Self-ordering electrochemical anodization is very simple and advantageous method including controllable pore structure with high aspect ratio and cost competitive fabrication. The potential of nanopores to mimic protein nanochannels in cell membranes which have single molecule sensitivity and selectivity and selectivity is critical toward the development of novel bio-inspired biosensors [91]. Anodic aluminum oxide is an excellent platform for the development of advanced, smart, simple, cost-effective sensing devices for numerous analytical applications. AAO has unique dimensions, geometry, and chemical composition which show characteristics responses when interacting with light. AAO is an outstanding platform for the fabrication of sensing devices with optical properties including reflectance, transmittance, absorbance, photoluminescence, chemiluminescence, and wave guiding. AAO chemical sensors and biosensors have been used in a broad range of application from gases, vapors, organic molecules, biomolecules (DNA, protein, antibodies) and, cells (viruses, bacteria, cancer cells) in air, water, and biological environment.

For the fabrication of highly ordered nanohole arrays, porous anodic alumina film is used as molds [92-95]. Al nanodot array is formed at the interface between the porous alumina film and the  $\text{SiO}_2$  film by a breakup of Al film due to completion of anodic oxidation. These

Al nanodots are useful for the application to quantum effect devices such as single electron memory nodes or quantum cellular automata devices [96].

## 8. REFERENCES

- G. E. J. Poinern, N. Ali, D. Fawcett, (2011) progress in nano-engineered anodic aluminum oxide membrane development, *Materials*, **4**: 487-526.
- H. Masuda, F. Fukuda, (1995) Ordered metal nanohole arrays made by a two-step replication of honeycomb structures of anodic alumina, *Science*, **268**: 1466-1468.
- J. Konieczny, L.A. Dobrzanski, K. Labisz, J. Duszczuk, (2004) The influence of cast method and anodizing parameters on structure and layer thickness of aluminium alloys, *Journal of Materials Processing Technology*, **157/158**: 718-723.
- L. Zaraska, G.D. Sulka, J. Szeremeta, M. Jaskuła, (2010) Porous anodic alumina formed by anodization of aluminum alloy (AA1050) and high purity aluminum, *Electrochimica Acta*, **55**: 4377-4386.
- M. Wu, U. Wen, Y. Lei, S. Ostendorp, K. Chen, G. Wild, (2010) Ultrathin alumina membranes for surface nanopatterning in fabricating quantum-sized nanodots, *Small*, **6**: 695-699.
- J. L. van Hemmen, S. B. S. Heil, J. H. Klootwijk, F. Roozeboom, C. J. Hodson, M. C. M. van de Sanden, W. M. M. Kessels, (2007) Plasma and thermal ALD of Al<sub>2</sub>O<sub>3</sub> in a commercial 200 mm ALD reactor, *Journal of The Electrochemical Society*, **154**: G165-G169.
- T. Aerts, I. D. Graeve, H. Terryn, (2010) Anodizing of aluminium under applied electrode temperature: Process evaluation and elimination of burning at high current densities, *Surface and Coatings Technology*, **204**: 2754-2760.
- M. Winterer, (2002) *Structure Of Nanocrystalline Materials*, Springer Series in Materials Science, Vol. 53. Berlin, Heidelberg: Springer-Verlag.
- M. Winterer, H. Hahn, (2003) Nanoceramics by chemical vapour synthesis, *Zeitschrift für Metallkunde*, **94**: 1084-1090.
- C. S. Blackman, X. Correig, V. Katko, A. Mozalev, I. P. Parkin, R. Alcubilla, T. Trifonov, (2008) Templated growth of tungsten oxide micro/nanostructures using aerosol assisted chemical vapour deposition, *Materials Letters*, **62**: 4582-4584.
- L. Sugiura, K. Shigenaka, F. Nakata, K. Hirahara, (1994) Misfit dislocation microstructure and kinetics of HgCdTe/CdZnTe under tensile and compressive stress, *Journal of Crystal Growth*, **145**: 547-551.
- A. A. Tahir, K. G. U. Wijayantha, S. S. Yarahmadi, M. Mazhar, V. McKee, (2009) Nanostructured  $\alpha$ -Fe<sub>2</sub>O<sub>3</sub> thin films for photoelectrochemical hydrogen generation, *Chemistry of Materials*, **21**: 3763-3772.
- J. Ohi, (2005) Hydrogen energy cycle: An overview, *Journal of Materials Research*, **20**: 3180-3187.
- X. C. Wu, Y. R. Tao, (2002) Growth of CdS nanowires by physical vapor deposition, *Journal of Crystal Growth*, **242**: 309-312.
- G. Sauer, G. Brehm, S. Schneider, K. Nielsch, R. B. Wehrspohn, J. Choi, H. Hofmeister, U. Gosele, (2002) Highly ordered monocrystalline silver nanowire arrays, *Journal of Applied Physics*, **91**: 3243-3247.
- L. Li, S. Pan, X. Dou, Y. Zhu, X. Huang, Y. Yang, G. Li, L. Zhang, (2007) Direct electrodeposition of Zn nanotube arrays in anodic alumina membranes, *The Journal of Physical Chemistry C*, **111(20)**: 7288-7291.
- J. R. V. Garcia, T. Goto, (2003) Chemical vapor deposition of iridium, platinum, rhodium and palladium, *Materials Transactions*, **44**: 1717-1728.
- M. Kumar, Y. Ando (2010) Chemical vapor deposition of carbon nanotubes: A review on growth mechanism and mass production, *Journal of Nanoscience and Nanotechnology*, **10**: 3739-3758.
- M. H. Siadati, T. L. Ward, J. Martus, P. Atanasova, C. Xia, R. W. Schwartz, (1997) Fabrication of Ag/Y<sub>2</sub>O<sub>3</sub> stabilized ZrO<sub>2</sub> composite films by metallorganic chemical vapour deposition, *Chemical Vapor Deposition*, **3**: 311-317.
- Y. C. Suia, B. Z. Cuib, R. Guardianc, D. R. Acostad, L. Martineza, R. Perez, (2002) Growth of carbon nanotubes and nanofibres in porous anodic alumina film, *Carbon*, **40**: 1011-1016.
- S. A. Steiner, T. F. Baumann, B. C. Bayer, R. Blyme, M. A. Worsley, W. J. Moberlychan, E. L. Shaw, R. Schlogl, A. J. Hart, S. Hoffmann, B. L. Wardle, (2009) Nanoscale zirconia as a nonmetallic catalyst for graphitization of carbon and growth of single- and multiwall carbon nanotubes, *Journal of the American Chemical Society*, **131**: 12144-12154.
- J. M. Kim, J. S. Park, K. T. Kim, (2010) Electrical conductivity and tensile properties of severely cold-worked Cu-P based alloy sheets, *Metals and Materials International*, **16**: 657-661.
- R. Sharma, S. W. Chee, A. Herzing, R. Miranda, P. Rez, (2011) Evaluation of the role of Au in improving catalytic activity of Ni nanoparticles for the formation of one-dimensional carbon nanostructures, *Nano Letters*, **11**: 2464-2471.
- E. Flahaut, C. Laurent, A. Peigney (2005) Catalytic CVD synthesis of double and triple-walled carbon nanotubes by the control of the catalyst preparation, *Carbon*, **43**: 375-383.
- S. C. Lyu, B. C. Liu, C. J. Lee, H. K. Kang, C. W. Yang, C. Y. Park, (2003) High-quality

- double-walled carbon nanotubes produced by catalytic decomposition of benzene, *Chemistry of Materials*, **15**: 3951-3954.
26. Q. Jiang, L. J. Song, H. Yang, Z. W. He, Y. Zhao, (2008) Preparation and characterization on the carbon nanotube chemically modified electrode grown in situ, *Electrochemistry Communications*, **10**: 424-427.
  27. J. M. Feng, R. Wang, Y. L. Li, X. H. Zhong, L. Cui, Q. J. Guo, F. Hou, (2010) One-step fabrication of high quality double-walled carbon nanotube thin films by a chemical vapor deposition process, *Carbon*, **48**: 3817-3824.
  28. H. J. Kim, E. Oh, J. Lee, D. S. Shim, K. H. Lee, (2011) Synthesis of carbon nanotubes with catalytic iron-containing proteins, *Carbon*, **49**: 3717-3722.
  29. S. H. Lim, Z. Q. Luo, Z. X. Shen, J. Y. Lin, (2010) Plasma-assisted synthesis of carbon nanotubes, *Nanoscale Research Letters*, **5**: 1377-1386.
  30. M. Kim, L. Gangloff, (2009) Growth of carbon nanotubes (CNTs) on metallic underlayers by diffusion plasma-enhanced chemical vapour deposition (DPECVD), *Physica E: Low-dimensional Systems and Nanostructures*, **41(10)**: 1763-1766.
  31. Electrodeposition of Indium Antimonide Nanowires in Porous Anodic Alumina Membrane, (2010) Published in-Micro/Nano Symposium (UGM) p1-4.
  32. M. Andres-Verges, C. Fernandez-Gonzalez, M. Martinez-Gallego, J. D. Solier, I. Cachadina, E. Matijevic, (2000) A new route for the synthesis of calcium-deficient hydroxyapatites with low Ca/P ratio: Both spectroscopic and electric characterization, *Journal of Materials Research*, **15**: 2526-2533.
  33. H. Gomez, D. Lincot, E. Dalchiele, G. Riveros, A. Cortes, (2007) Presentation: Oral at E-MRS Fall Meeting, Symposium B.
  34. R. Chen, D. Xu, G. Guo, L. Gui, (2002) Silver telluride nanowires prepared by dc electrodeposition in porous anodic alumina templates, *Journal of Materials Research*, **12**: 2435-2438.
  35. J. Sarkar, G. G. Khan, A. Basumallick, (2007) Nanowires: properties, applications and synthesis via porous anodic aluminium oxide template, *Bulletin of Material Science*, **30**: 271-290.
  36. R. Inguanta, S. Piazza, C. Sunseri, (2008) Novel procedure for the template synthesis of metal nanostructures, *Electrochemistry Communications*, **10**: 506-509.
  37. R. Inguanta, M. Butera, C. Sunseri, S. Piazza, (2007a) Fabrication of metal nano-structures using anodic alumina membranes grown in phosphoric acid solution: Tailoring template morphology, *Applied Surface Science*, **253**: 5447-5456.
  38. G. Ferrara, R. Inguanta, S. Piazza, C. Sunseri, (2008b) Nanostructures fabrication by template deposition into anodic alumina membranes, *Patent RM2008A000341*.
  39. R. Inguanta, S. Piazza, C. Sunseri, (2008b) Template electrosynthesis of aligned Cu<sub>2</sub>O nanowires: Part I. Fabrication and characterization, *Electrochim. Acta*, **53**: 6504-6512.
  40. G. Wolfowicz, A. M. Tyryshkin, R. E. George, H. Riemann, N. V. Abrosimov, P. Becker, H. J. Pohl, M. L. W. Thewalt, S. A. Lyon, J. J. L. Morton, (2013) Atomic clock transitions in silicon-based spin qubits, *Nature Nanotechnology*, **8**: 561-564.
  41. Y. Sun, B. T. Mayers, Y. Xia, (2002) Template-engaged replacement reaction: A one-step approach to the large-scale synthesis of metal nanostructures with hollow interiors, *Nano Letters*, **2**: 481-485.
  42. T. Hanoka, H. P. Kormann, M. Kroll, T. Szwajkowski, G. Schmid, (1998) Three-dimensional assemblies of gold colloids in nanoporous alumina membranes, *European Journal of Inorganic Chemistry*, **1998(6)**: 807-812.
  43. J. Xu, J. Xia, J. Wang, J. Shinar, Z. Lin, (2006) Quantum dots confined in nanoporous alumina membranes, *Applied Physics Letters*, **89**: 133110-133113.
  44. R. Gaggiano, P. Moriame, M. Biesemans, I. D. Graeve, H. Terryn, (2011) Influence of SiO<sub>2</sub>/Na<sub>2</sub>O ratio and temperature on the mechanism of interaction of soluble sodium silicates with porous anodic alumina, *Surface and Coatings Technology*, **206**: 1269-1276.
  45. I. Seo, C. W. Kwon, H. H. Lee, Y. S. Kim, K. B. Kim, T. S. Yoon, (2009) Completely filling anodic aluminum oxide with maghemite nanoparticles by dip coating and their magnetic properties, *Electrochemical and Solid-State Letters*, **12**: K59-K62.
  46. L. Yao, J. H. Liu, M. Yu, S. M. Li, H. Wu, (2010) Formation and capacitance properties of Ti-Al composite oxide film on aluminum, *Transactions of Nonferrous Metals Society of China*, **20**: 825-830.
  47. J. Lee, J. Choi, J. Lee, S. K. Choi, H. D. Chun, (2005) Improved voltage margins using linear error-correcting codes in resistor-logic demultiplexers for nanoelectronics, *Nanotechnology*, **16**: 1449-1453.
  48. C. M. Crego, D. N. Reinhoudt, (2008) Self-assembling nanoparticles at surfaces and interfaces, *Chem Phys Chem*, **9(1)**: 20-42.
  49. P. Y. Silvert, R. H. Urbina, N. Duvauchelle, V. Vijaykrishnan, K. T. Elhsissen, (1996) Preparation of colloidal silver dispersions by the polyol process. Part 1—Synthesis and characterization, *Journal of Materials Chemistry*, **6**: 573-577.
  50. P. A. Libby, (1952) An experimental investigation of the isothermal laminar boundary layer on a

- porous flat plate, *Journal of the Aeronautical Science*, **19(2)**: 127-134.
51. Y. C. Choi, J. Kim, J. K. Han, S. D. Bu, (2006) Alumina-membrane-based growth of functional PbO<sub>2</sub> and Pb (Zr, Ti) O<sub>3</sub> metal-oxide nanowires by spin coating, *Journal of the Korean Physical Society*, **49**: S523-S528.
  52. P. Dorenbos, (2003) Exchange and crystal field effects on the 4f<sup>n-1</sup>5d levels of Tb<sup>3+</sup>, *Journal of Physics: Condensed Matter*, **15**: 6249-6268.
  53. G. Xomeritakis, N. G. Liu, Z. Chen, Y. B. Jiang, R. Kohn, P. E. Johnson, C. Y. Tsai, P. B. Shah, S. Khalil, S. Singh, C. J. Brinker, (2007) Anodic alumina supported dual-layer microporous silica membranes, *Journal of Membrane Science*, **287**: 157-161.
  54. D. Linden, T. B. Reddy, (2002) *Handbook of Batteries*, New York: Mcgraw hill.
  55. J. F. Lei, (1997) Advances in Thin Film Sensor Technologies for Engine Applications, NASA Technical Memorandum, 107418.
  56. C. DellaCorte, J. A. Fellenstein, P. A. Benoy, (1998) Evaluation of Advanced Solid Lubricant Coatings for Foil Air Bearings Operating at 25 and 500°C, NASA/TM-206619.
  57. M. Tian, S. Xu, J. Wang, N. Kumar, E. Wertz, Q. Li, P. M. Campbell, M. H. W. Chan, T. E. Mallouk, (2005) Penetrating the oxide barrier in situ and separating freestanding porous anodic alumina films in one step, *Nano Letters*, **5**: 697-703.
  58. J. Oh, Y. Tak, J. Lee, (2004) Electrodeposition of Cu<sub>2</sub>O of Cu<sub>2</sub>O using nanoporous alumina template, *Electrochemical and Solid-State Letters*, **7**: C27-C30.
  59. L. X. Shao, K. H. Chang, T. H. Chung, B. H. Tseng, H. L. Hwang, (2003) Steps toward industrialization of Cu-III-VI<sub>2</sub> thin-film solar cells: A novel full in-line concept, *Journal of Physics and Chemistry of Solids*, **64**: 1505-1509.
  60. C. J. Wu, H. N. Huang, F. H. Lu, (2005) Phase transformations in copper oxide nanowires, *Journal of Vacuum Science & Technology B*, **23**: 2557-2560.
  61. S. Wang, G. J. Yu, J. L. Gong, D. Z. Zhu, H. H. Xia (2007) Large-area uniform nanodot arrays embedded in porous anodic alumina, *Nanotechnology*, **18**: 015303-015306.
  62. D. D. Sung, M. S. Choo, J. S. Noh, W. B. Chin, W.S. Yang (2006) A new fabrication method of aluminum nanotube using anodic porous alumina film as a template, *Bulletin of the Korean Chemical Society*, **27**: 1159-1163.
  63. C. C. Lu, Y. S. Huang, J. W. Huang, C. K. Chang, S. P. Wu, (2010) A macroporous TiO<sub>2</sub> oxygen sensor fabricated using anodic aluminium oxide as an etching mask, *Sensors*, **10**: 670-683.
  64. S. Z. Chu, K. Wada, S. Inoue, S. I. Todoroki, Y. K. Takahashi, K. Hono, (2002) Fabrication and characteristics of ordered ni nanostructures on glass by anodization and direct current electrodeposition, *Chemistry of Materials*, **14**: 4595-4602.
  65. Y. Yang, H. Chen, Y. Mei, J. Chen, X. Wu, X. Bao, (2002) CdS nanocrystallites prepared by chemical and physical templates, *Acta Materialia*, **50**: 5085-5090.
  66. A. V. Kukhta, G. G. Gorokh, E. E. Kolesnik, A. I. Mitkovets, M. I. Taoubi, Y. A. Koshin, A. M. Mozalev, (2002) Nanostructured alumina as a cathode of organic light-emitting devices, *Surface Science*, **507-510**: 593-597.
  67. H. J. Wang, C. W. Zou, B. Yang, H. B. Lu, C. X. Tian, H. J. Yang, M. Li, C. S. Liu, D. J. Fu, J. R. Liu, (2009) Electrodeposition of tubular-rod structure gold nanowires using nanoporous anodic alumina oxide as template, *Electrochemistry Communications*, **11**: 2019-2022.
  68. G. J. Hutchings (2008) Nanocrystalline gold and gold palladium alloy catalysts for chemical synthesis, *Chemical Communications*, **10**: 1148-1164.
  69. S. Panigrahi, S. Basu, S. Praharaj, S. Pande, S. Jana, A. Pal, S. K. Ghosh, T. Pal, (2007) Synthesis and size-selective catalysis by supported gold nanoparticles: Study on heterogeneous and homogeneous catalytic process, *The Journal of Physical Chemistry C*, **111**: 4596-4605.
  70. M. Nishizawa, V. P. Menon, C. R. Martin, (1995) Metal nanotubule membranes with electrochemically switchable ion-transport selectivity, *Science*, **268**: 700-702.
  71. M. Delvaux, S. D. Champagne, (2003) Immobilisation of glucose oxidase within metallic nanotubes arrays for application to enzyme biosensors, *Biosensors and Bioelectronics*, **18**: 943-951.
  72. C. R. Martin, P. Kohli, (2003) The emerging field of nanotube biotechnology, *Nature Reviews Drug Discovery*, **2**: 29-37.
  73. S. Y. Chou, P. R. Krauss, W. Zhang, L. Guo, L. Zhuang, (1997) Sub-10 nm imprint lithography and applications, *Journal of Vacuum Science & Technology B*, **15**: 2897-2904.
  74. Y. G. Guo, L. J. Wan, C. F. Zhu, D. L. Yang, D. M. Chen, C. L. Bai, (2003) Ordered Ni-Cu nanowire array with enhanced coercivity, *Chemistry of Materials*, **15**: 664-667.
  75. S. R. N. Pena, R. G. Freeman, B. D. Reiss, L. He, D. J. Pena, I. D. Walton, R. Cromer, C. D. Keating, M. J. Natan, (2001) Submicrometer metallic barcodes, *Science*, **294**: 137-141.
  76. S. Iijima, (1991) Helical microtubules of graphitic carbon, *Nature*, **354**: 56-58.
  77. P. Ball, (2001) Carbon nanotubes in Nature, *Nature*, **2**: 1,6.
  78. M. A. Olshavsky, A. N. Goldstein, A. P. Alivisatos, (1990) Organometallic synthesis of gallium-

- arsenide crystallites, exhibiting quantum confinement, *Journal of the American Chemical Society*, **112**: 9438-9439.
79. R. M. Penner, (2000) Hybrid electrochemical/chemical synthesis of quantum dots, *Accounts of Chemical Research*, **33**: 78-86.
  80. A. Henglein, (1988) Mechanism of reactions on colloidal microelectrodes and size quantization effects, *Topics in Current Chemistry*, **143**: 113.
  81. Y. Xia, P. Yang, Y. Sun, Y. Wu, B. Mayers, B. Gates, Y. Yin, F. Kim, H. Yan, (2003) One-dimensional nanostructures: Synthesis, characterization, and applications, *Advanced Materials*, **15**: 353-389.
  82. A. I. Hochbaum, P. Yang, (2010) Semiconductor nanowires for energy conversion, *Chemical Reviews*, **110**: 527-546.
  83. N. Wang, Y. Cai, R. Q. Zhang, (2008) Growth of nanowires, *Materials Science and Engineering: R*, **60**: 1-51.
  84. E. Gyorgy, G. Socol, E. Axente, I. N. Mihailescu, C. Ducu, S. Ciuca, (2005) Anatase phase TiO<sub>2</sub> thin films obtained by pulsed laser deposition for gas sensing applications, *Applied Surface Science*, **247**: 429-433.
  85. H. S. Kim, W. T. Moon, Y. K. Jun, S. H. Hong, (2006) High H<sub>2</sub> sensing performance in hydrogen trititanate-derived TiO<sub>2</sub>, *Sens. Actuators B: Chemical*, **120**: 63-68.
  86. I. Sayago, E. Terrado, E. Lafuente, M. C. Horrillo, W. K. Maser, A. M. Benito, R. Navarro, E. P. Urriolabeitia, M. T. Martinez, J. Gutierrez, (2005) Hydrogen sensors based on carbon nanotubes thin films, *Synthetic Metals*, **148(1)**: 15-19.
  87. C. S. Huang, B. R. Huang, Y. H. Jang, M. S. Tsai, C. Y. Yeh, (2005) Three-terminal CNTs gas sensor for N<sub>2</sub> detection, *Diamond and Related Materials*, **14**: 1872-1875.
  88. M. Consales, S. Campopiano, A. Cutolo, M. Penza, P. Aversa, G. Cassano, M. Giordano, A. Cusano (2006) Carbon nanotubes thin films fiber optic and acoustic VOCs sensors: Performances analysis, *Sens. Actuators B: Chemical*, **118**: 232-242.
  89. M. D. Dickey, E. A. Weiss, E. J. Smythe, R. C. Chiechi, F. Capasso, G. M. Whitesides, (2008) Fabrication of arrays of metal and metal oxide nanotubes by shadow evaporation, *ACS Nano*, **2**: 800-808.
  90. Z. Dai, H. Ju, (2012) Bioanalysis based on nanoporous materials, *Trends in Analytical Chemistry*, **39**: 149-162.
  91. A. E. Muniz, A. Merkoci, (2012) Nanochannels preparation and application in biosensing, *ACS Nano*, **6**: 7556-7583.
  92. F. Keller, M. S. Hunter, D. L. Robinson, (1953) Structural features of oxide coatings on aluminum, *J. The Electrochemical Society*, **100**: 411-419.
  93. G. L. Hornyak, C. J. Patrissi, C. R. Martin, (1997) Fabrication, characterization, and optical properties of gold nanoparticle/porous alumina composites: The nonscattering maxwell-garnett limit, *The Journal of Physical Chemistry B*, **101**: 1548-1555.
  94. S. Shingubara, O. Okino, Y. Sayama, H. Sakaue, T. Takahagi, (1997) Ordered two-dimensional nanowire array formation using self-organized nanoholes of anodically oxidized aluminum, *Japanese Journal of Applied Physics*, **36**: 7791-7796.
  95. S. Shingubara, O. Okino, Y. Murakami, H. Sakaue, T. Takahagi, (2001) Fabrication of nanohole array on Si using self-organized porous alumina mask, *Journal of Vacuum Science & Technology B*, **19**: 1901-1904.
  96. I. Amlani, A. O. Orlov, R. K. Kummamuru, G. H. Bernstein, C. S. Lent, G. L. Snider, (2000) Experimental demonstration of a leadless quantum-dot cellular automata cell, *Applied Physics Letters*, **77**: 738-740.

#### \*Bibliographical Sketch



Dr. Naveen Verma has achieved M.Sc chemistry from M. D. University, Rohtak Haryana. He has obtained his Ph. D degree from Dept. of chemistry, M D University, Rohtak, Haryana. He has published 10 research papers in reputed International journals and also presented his papers in many national conferences. He has visited university of Polytechnica Valencia, Spain in the frame work of an international project sanctioned by European Union. He has also 5 year teaching experience as Assistant Professor Chemistry, in Department of Chemistry M. D. University, Rohtak, Haryana.